Transverse Shear Oscillator Investigation of Boundary Lubrication in Weakly Adhered Films

J. Léopoldès* and X. Jia†

Université Paris Est, Laboratoire de Physique des Matériaux divisés et Interfaces CNRS FRE 3300, 5 Bd Descartes, 77454 Marne la Vallée cedex 2, France

(Received 11 June 2010; revised manuscript received 16 October 2010; published 20 December 2010)

We investigate the boundary lubrication in weakly adhered molecularly thin films deposited between a sphere and a plane, below the sliding threshold. The shear contact stiffness and interfacial dissipation at the micrometer scale are determined with a high-frequency quartz oscillator. Two distinct behaviors are found as a function of the shear oscillation: a linear viscoelastic response at low amplitude and a nonlinear frictional microslip at high amplitude. A friction model is proposed to analyze the data, which allows evaluating the shear strength, the friction coefficient, and the interfacial viscosity at different solid interfaces under low load.

DOI: 10.1103/PhysRevLett.105.266101 PACS numbers: 68.35.Gy, 43.35.+d

Introduction.—Thin films deposited on solid surfaces are extensively used to tailor a broad range of properties such as optical transmission, electronic transport, adhesion, or lubrication. As the thickness of the thin film h is decreased down to a characteristic length scale relevant for a given physical mechanism, some confinement effects take place [1]. Furthermore, the nonlinear mechanical behavior may come into play due to large shear strains $\varepsilon_T \sim U_T/h$ at a given shear amplitude U_T [2]. Highlighting the mechanisms responsible for the nonlinear properties of thin films is essential for understanding phenomena such as dewetting [3] and solid friction [4].

Indeed, thin films highly confined between flat contacting solid surfaces under shear ($h \sim 1$ nm) control the friction dynamics of the interface [5]. In such a boundary lubrication regime, the static friction threshold F_T is commonly described by the classical Amontons-Coulomb laws, $F_T = \mu N$ with N the normal load and μ the coefficient of friction [6]. Following Tabor, the threshold can be alternatively expressed as $F_T = \sigma_s \Sigma_r$ where Σ_r is the real contact area proportional to N and σ_s is the interfacial shear strength. Baumberger and Caroli have recently shown that σ_s corresponds to the yield stress of the interfacial layer (junction) consisting of a molecularly disordered medium with $h \sim 1$ nm [4]. At low shear level the interfacial layer is pinned and responds to shear elastically; beyond the threshold it flows plastically due to the structural rearrangements at the nanometric scales within the junction. On the other hand, it has been shown that the adhesion may play a crucial role in the static threshold. Under low normal load, the modified Coulomb law reads $F_T = F_0 + \mu N$ where F_0 is the shear threshold under zero load [7]. However, the physical mechanisms that precede the threshold F_T and the interplay between friction and adhesion remain poorly understood [8] due to the lack of experimental data.

Alternatively, the frictional dynamics can be studied with the sphere-plane geometry. For a loaded nonadhesive contact between a smooth sphere and a plane surface, Mindlin derived a relationship between the shear displacement and the tangential force [9]. When the amplitude of the shear displacement increases, a micro-slip annulus grows from the edge of the contact area towards the center, until the macroscopic sliding is reached and the full contact slips. For an adhesive contact, the shear failure during the incipient stages of sliding friction involves generally a stiction process: a similar zone of microslip develops whose growth is controlled by a complex interplay between friction energy and adhesion [10].

In this Letter, we address the above issues by investigating the shear oscillatory response of solid interfaces coated with weakly adhesive and ultrathin films (~ 1 nm), within the framework of the friction dynamics. The shear contact stiffness and interfacial dissipation before the sliding threshold are determined using the sphere-plane geometry by a resonance method at the MHz frequency [11,12]. This work may be relevant for the mechanical behavior and the vibrational dynamics of granular materials [13]. It is also appropriate for the development of microelectromechanical systems where the friction related to the adhesion between solids at low load is a major issue. In this context, our findings would be of practical importance for better understanding the high-frequency tribology [11,12].

Experiments.—Our experimental setup is depicted Fig. 1(a). The probe in contact with the coated quartz resonator is composed of a calibrated steel sphere of diameter $2R = 2$ mm. To minimize the rotation of the sphere under shear oscillation, the sphere is mounted on a glass capillary vertically aligned on the center of the quartz. The normal load N applied to the interface is 2 mN. The rms roughness of the sphere is about 10 nm as measured by atomic force microscopy on a surface area of $20 \times 20\ \mu\text{m}^2$ and that of the quartz is about 1 nm over $10 \times 10\ \mu\text{m}^2$.

For preparing the interfaces with the monolayers, the metallized (Au) quartz surface is adsorbed with thiol solutions of mercaptoundecanoic acid or octadecanethiol,

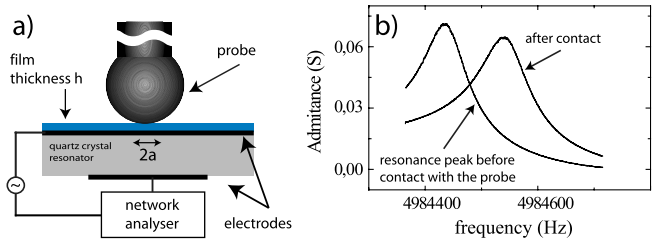

FIG. 1 (color online). (a) Sketch of the sphere-plane geometry using a quartz resonator. (b) Typical alteration of the resonance peak after contact with the probe.

resulting in well packed monolayers terminated, respectively, with −COOH ($h = 1$ nm) and −CH3 ($h = 2$ nm) groups, providing a wide range of interfacial energies [14]. These monolayers have a simple hydrocarbon chain, with essentially the same rheological properties as other ubiquitious hydrocarbon films found in the literature. Here the surfaces coated with the solid lubricants −CH3 and −COOH are referred to as lubricated, while the unaltered Au and Steel interfaces are referred to as unlubricated or "bare." Two systems of interfaces adsorbed with a cured polydimethysiloxane (PDMS) brush (∼ 18 and 100 nm) are also prepared for comparison. The PDMS films are adsorbed on the surface by spin coating from heptane solutions, and cured overnight at 90 °C. The quartz resonator is mounted in a home made cell and all experiments are conducted at 40 °C under ambient humidity inside an oven.

The quartz resonator in shear thickness mode is driven by a network analyzer with the oscillation amplitude U_T varying roughly from 0.1 to 5 nm estimated by $U_T = CQV$ with $C = 1.3$ pm/V, Q the quality factor of the resonance peak, and V the applied voltage [15]. Before each measurement, the resonator is left in the oven for 30 min until thermal stabilization. Figure 1(b) displays the typical admittance spectra obtained at resonance ∼5 MHz before and after the probe is put in contact with the quartz using a microcontrol element. For every contact, the spectral responses associated with four cycles of excitation from low to high amplitude are recorded. The response to the first cycle is different from the others (20% error). This dispersion frequently encountered in solid friction [4] stems from a large number of configurations of interfacial pinning sites. When the unsheared junctions are created by bringing the two solids in contact, the initial state of the interface is not reproducible. To the contrary, the first cycle of shearing allows one to prepare the interface in a controlled way [4]. The recorded spectrum for the data analysis is the averaged response over the next three well-correlated cycles of excitation, which is in turn averaged on measurements performed with two other different contacts.

The alteration of the resonance peak after the contact between the sphere and the quartz consists of the shift Δf (> 0) of the resonance frequency f_0 and the increase of the inverse quality factor ΔQ^{-1}. They can be related, respectively, to the interfacial stiffness $k_T = 4\pi(MK)^{1/2}\Delta f$ and dissipation $\Delta W_{\text{loss}} = \pi K U_T^2 \Delta Q^{-1}$ where M and K are the effective mass and stiffness of the quartz and U_T is the amplitude of shear displacement [12]. Figure 2(a) illustrates both k_T and ΔQ^{-1} measured versus U_T for the interface adsorbed with the thick PDMS brush $h \sim 100$ nm. $k_T (= G'\pi a^2/h)$ and $\Delta Q^{-1} (= G''\pi a^2/hK)$ (with G' and G'' the elastic and dissipative modulus) are independent of U_T, indicative of a linear response over the available amplitude range. Such behavior arises probably from the linear viscoelastic properties of the polymer layer bonded at the PDMS-probe interface, expected at the maximum shear strain $\varepsilon_T \sim 5\%$ [12]. However, for thinner film $h = 18$ nm, the stiffness decreases for shear amplitudes larger than $U_T \sim 1$ nm. We illustrate this softening by plotting in the inset of Fig. 2(b) the elastic moduli of the 100 nm and 18 nm films versus the effective shear strain $\varepsilon_{\text{eff}} = U_T/h$, normalized by the plateau value G' when $\varepsilon_{\text{eff}} \to 0$. Nonlinear behavior of these thin films occurs for $\varepsilon_{\text{eff}} > 10\%$, corresponding to the complex rheological features intermediate between the bulk and boundary properties [16]. Here we will focus on the boundary lubrication regime of the thin films. For the PDMS films less than 10 nm, spinodal decomposition arises after spin coating, preventing the accurate analysis. We therefore pursue our study with the self assembled monolayers.

The interface between a −CH3 coated quartz and the steel sphere exhibits a similar rheological behavior versus the shear amplitude. As shown in Fig. 2(c), we find that k_T and ΔQ^{-1} remain roughly constant at low amplitude as in the case with the thick adsorbed film [Fig. 2(a)]. However, k_T decreases about 30% at high amplitude ($U_T > U_c \sim 1$ nm), indicating a nonlinear regime, while the dissipation increases simultaneously by a factor of 2. Such nonlinear

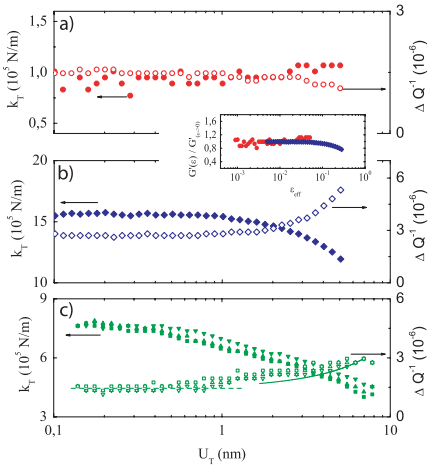

FIG. 2 (color online). Measured shear stiffness and inverse of quality factor versus shear amplitude at load $N = 2$ mN. (a) For a PDMS brush of $h = 100$ nm. (b) For a PDMS brush of $h = 18$ nm. Inset: Normalized elastic modulus versus shear strain (see text). (c) For a quartz coated with the −CH3 monolayer, three successive runs of measurements are made. The dotted and solid lines correspond to the linear dissipation and ΔW (see text), respectively.

behavior is repeatable for successive shear experiments and does not arise from friction-induced monolayer damage or surface melting, due to the small shear amplitudes and the metals of high melting temperature used here [17]. The nonlinear behavior shown in Fig. 2(c) is also observed at the other interfaces. We find that the shear contact stiffness is only slightly altered when the bare quartz is covered by a −COOH film [Fig. 3(a)]. However, these systems exhibit quite different interfacial dissipation [Fig. 3(b)].

Analysis and discussion.—Linear and nonlinear regimes have been reported in the oscillating experiments along different interfaces [9,18,19]. Unlike the previous works, the present experimental results demonstrate the existence of a finite oscillation amplitude U_c below which the rheological response is linear, suggesting strongly the adhesive nature of the contact. In order to account for the two distinct regimes observed, we propose a modified friction model based on the Mindlin theory [9]. As a function of the shear displacement U_T, we write the tangential force F_T as

$$F_T = k_E U_T \quad \text{for } U_T < U_c \tag{1a}$$

$$F_T = F_0 + F_M(U_T) \quad \text{for } U_T > U_c \tag{1b}$$

where k_E is the constant shear stiffness associated with a bonded contact in the linear regime and F_0 is a shear threshold under zero normal load N. F_M is a frictional term used to describe the nonlinear response for the sphere-plane geometry [9], $F_M = \mu N\{1 - [1 - 16(G^* a)U_T/(3\mu N)]^{3/2}\}$. Here μ is the coefficient of friction, G^* is the reduced shear modulus and a is the radius of the contact area. When increasing F_M up to $\geq \mu N$, the microslip annulus covers the whole contact area and the full sliding between the sphere and the plane occurs. Thus, Eq. (1b) is formally equal to the above modified Coulomb law at the sliding threshold. This model may allow describing qualitatively both the amplitude-dependent shear contact stiffness k_T and the frictional dissipation ΔQ^{-1} (see below).

We first evaluate the radius a of the contact area in the presence of adhesion. For low shear amplitude, the Mindlin theory predicts similar normal k_N and tangential k_T contact stiffness, $k_N \sim k_T = 8G^* a$ [9]. Such scaling also holds for adhesive contacts where a depends both on normal load and adhesion, as given by the Johnson-Kendall-Roberts model [9]. In this work, we assume that $k_T \sim k_E$ at low amplitude [Fig. 3]. Using the reduced shear and Young moduli for the steel and quartz materials, $G^* = 12$ GPa and $E^* = 67$ GPa, we can estimate the contact radius between the sphere and various surfaces: $a_{\text{Bare}} \sim 15\ \mu\text{m} \geq a_{\text{COOH}} \sim 14\ \mu\text{m} > a_{\text{CH3}} \sim 7.5\ \mu\text{m}$. Using the different interfacial energies, $\gamma_{\text{Au-Steel}} \sim 0.2$ N/m $\geq \gamma_{\text{COOH-Steel}} \sim 0.16$ N/m $> \gamma_{\text{CH3-Steel}} \sim 0.07$ N/m, the JKR model predicts the respective contact, $a_{\text{Au-Steel}} \sim 5.5\ \mu\text{m} \geq a_{\text{COOH-Steel}} \sim 5.2\ \mu\text{m} > a_{\text{CH3-Steel}} \sim 4.5\ \mu\text{m}$, which is fairly consistent with the experimental results.

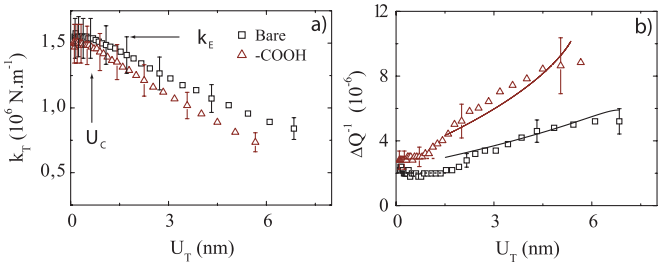

FIG. 3 (color online). Measured shear stiffness (a) and inverse quality factor (b) for the interfaces with a bare quartz and a −COOH coated quartz at load $N = 2$ mN. The dotted and solid lines correspond to the linear dissipation and ΔW (see text), respectively.

On the other hand, a shear threshold may be estimated with $F_0 \sim k_E U_C$ (~1 nm) [Fig. 3(a)] which is $F_{0(\text{Bare})} \sim 0.8$ mN, $F_{0(\text{COOH})} \sim 0.8$ mN, and $F_{0(\text{CH3})} \sim 0.4$ mN, respectively. Using a surface equal to the contact area deduced from the shear stiffness, we calculate a shear strength $\sigma_0 \sim F_0/\pi a^2$ of the order of 1 MPa, which depends little on the van der Waals forces responsible for adhesion. This value is close to that obtained previously by Briscoe and Evans on organic monolayers equivalent to our lubricated surfaces [7]. Indeed, for a given contact area A, the above modified Coulomb law can be expressed in terms of the shear strength $\sigma_T = F_T/A = \sigma_0 + \mu P$. Here P is the normal pressure and σ_0 is the shear strength under zero load: in the vicinity of U_C the interfacial layer could weaken via plastic deformation as in amorphous media [4,7]. Clearly, further studies are required to uncover the underlying physics for this crossover.

The nonlinear regime observed at high amplitude, when U_T is larger enough than U_C, is ascribed to friction characterized by the friction coefficient μ. To compare the experimental results with the Mindlin-like model [Eq. (1b)], we replot in Fig. 4 the elastic response $F_T = k_T U_T$ versus U_T via the shear stiffness k_T obtained from Figs. 2(c) and 3(a). For $U_T > 2U_C$ in the frictional regime, k_T corresponds to the slope of the line connecting the limit points (F_T, U_T) of the hysteresis loop [9]. Figure 4 shows that the ultrasonic experiments are below the sliding threshold between the sphere and the substrate since the curves F_T versus U_T do not reach the plateau. Fitting Eq. (1b) provides both μ and the product $G^* a$. The contact radius a (~ 10 μm) deduced from the latter agrees well with that obtained from k_E, which is consistent with the above description on the adhesive contact. As expected, adding a monolayer decreases the coefficient of friction: $\mu_{\text{bare}} \approx 2.4 > \mu_{\text{COOH}} \approx 1.7 \sim \mu_{\text{CH3}} \approx 1.7$, due the lubrication effect. The absolute values of the friction coefficient appear higher than usual ones. This may be related to the low load measurement for which the increase of μ is frequently observed [6]. Also, the deviation of the Mindlin model is expected when applied to small-amplitude shear [18,19].

Let us now investigate the dissipative responses within the framework of the above model, using the same set of fit parameters obtained from the elastic responses. As described above, two regimes are considered. For $U_T < U_c$,

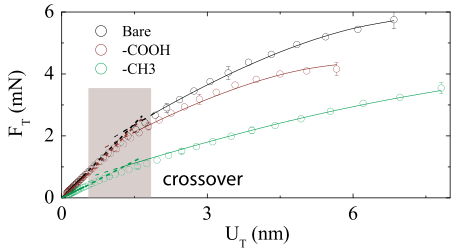

FIG. 4 (color online). Fits by Eq.(1) to the shear force-displacement responses for various interfaces.

we observe a linear regime, ascribed to the viscoelastic dissipation, $\Delta W_{\mathrm{vis}}(U_T) = (\pi a^2/h)2\pi f_0 \eta_{\mathrm{eff}} U_T^2$ with h the thickness of the interfacial film and η_{eff} the effective viscosity. Note that the loss by acoustic radiation into the sphere via the contact area a ($\sim 10\ \mu$m) should be negligible here since it is proportional to λ/a with a shear wavelength λ ($\sim 600\ \mu$m) in the steel sphere [20]. For $U_T > U_c$, the dissipation is determined by an interplay between a viscoelastic loss $\sim\Delta W_{\mathrm{vis}}(U_T)$ and a nonlinear frictional loss due to the microslip, $\Delta W = \Delta W_{\mathrm{vis}}(U_T) + \Delta W_{\mathrm{fric}}(F_T - F_0)$. The second term ΔW_{fric} corresponds to the Mindlin model [6], but the contribution of a shear threshold ($\sim F_0$) is removed from the tangential force F_T.

In the linear viscoelastic regime, an interfacial thickness $h \sim 1$ nm leads to an effective viscosity $\eta_{\mathrm{eff}} \sim 1$–$2$ mPa $\cdot$ s, comparable to that of linear short-chains alkanes [21] having the same structure as our monolayers. For the lubricated surfaces, this suggests that the interfacial dissipation would arise from the deposited monolayers. However, for the hydrophilic bare and $-$COOH covered surfaces, the interfacial capillary condensation might occur [13], providing a similar viscosity $\eta_{\mathrm{water}} \sim 1$ mPa $\cdot$ s. In the nonlinear regime, we derive the corresponding dissipation ΔW by computing ΔW_{fric} with the values a, F_0, and μ fitted above from the elastic responses. The computed dissipations are shown in Figs. 2(c) and 3(b). The agreement between the experimental data and the calculation is fairly good. This supports further the proposed scenario.

Conclusion.—Our experiments reveal a crossover, versus shear amplitude, of the elastic and dissipative responses of lubricated interfaces before the sliding threshold. Such behavior is likely due to the softening arising from nanometric adsorbed films and is analyzed within the framework of a Mindlin-like friction model with a shear threshold under zero load. The qualitative agreement between the experiments and the model indicates that the linear viscoelastic regime at low amplitude is determined by the properties of the contact, while the nonlinear regime at high amplitude is dominated by the frictional microslip initiated by the yielding of the interfacial film at the edges of the contact.

We believe that this work is useful to bridge two different approaches for studying the boundary lubrication in the presence of adhesion, namely, the solid friction picture and the fracture scenario [10]. We should learn in more details about the transition behavior under a vacuum environment, by a better characterization of the spatial heterogeneity of various monolayers.

We thank L. Bureau, Ch. Caroli, A. Chateauminois, and C. Frétigny for stimulating discussions and E. Drockenmuller for providing us with the PDMS brushes.

*julien.leopoldes@univ-mlv.fr
†jia@univ-mlv.fr

[1] E. Vidal-Russell and N. E. Israeloff, Nature (London) **408**, 695 (2000); H. Ogi *et al.*, Phys. Rev. Lett. **98**, 195503 (2007).
[2] G. Reiter *et al.*, J. Chem. Phys. **101**, 2606 (1994).
[3] K. Dalnoki-Veres *et al.*, Phys. Rev. E **59**, 2153 (1999).
[4] T. Baumberger and C. Caroli, Adv. Phys. **55**, 279 (2006).
[5] M. H. Müser, L. Wenning, and M. O. Robbins, Phys. Rev. Lett. **86**, 1295 (2001).
[6] F. P. Bowden and D. Tabor, *The Friction and Lubrication of Solids* (Oxford University Press, Oxford, 1958).
[7] B. J. Briscoe and D. C. B. Evans, Proc. R. Soc. A **380**, 389 (1982); A. M. Homola *et al.*, J. Tribol. **111**, 675 (1989).
[8] S. M. Rubinstein, G. Cohen, and J. Fineberg, Phys. Rev. Lett. **96**, 256103 (2006).
[9] K. L. Johnson, *Contact Mechanics* (Cambridge University Press, New York, 1985).
[10] M. Barquins, Wear **158**, 87 (1992); A. R. Savkoor and G. A. D. Briggs, Proc. R. Soc. A **356**, 103 (1977); K. L. Johnson, Proc. R. Soc. A **453**, 163 (1997); A. Chateauminois, C. Fretigny, and L. Olanier, Phys. Rev. E **81**, 026106 (2010).
[11] G. L. Dybwad, J. Appl. Phys. **58**, 2789 (1985); B. Borowsky *et al.*, J. Appl. Phys. **90**, 6391 (2001); S. Berg and D. Johannsmann, Phys. Rev. Lett. **91**, 145505 (2003).
[12] J. Léopoldès and X. Jia, Europhys. Lett. **88**, 34001 (2009).
[13] L. Bocquet *et al.*, Nature (London) **396**, 735 (1998); J. R. Royer *et al.*, Nature (London) **459**, 1110 (2009); A. Castellanos, Adv. Phys. **54**, 263 (2005); E. Somfai *et al.*, Phys. Rev. E **75**, 020301 (2007).
[14] C. D. Bain *et al.*, J. Am. Chem. Soc. **111**, 321 (1989).
[15] B. Borovski, B. L. Mason, and J. Krim, J. Appl. Phys. **88**, 4017 (2000); D. Johannsmann and L. O. Heim, J. Appl. Phys. **100**, 094505 (2006). The order of displacements corresponds to such kind of piezoelectric crystals, but quantitative shear amplitude could be measured with a Doppler velocity interferometer.
[16] H. W. Hu and S. Granick, Science **258**, 1339 (1992).
[17] B. D. Dawsons, S. M. Lee, and J. Krim, Phys. Rev. Lett. **103**, 205502 (2009); D. A. Hook *et al.*, J. Appl. Phys. **104**, 034303 (2008). The work done by frictional force per unit surface is $W \sim k_T(U_T)^2/A \sim 0.1$ J/m^2 with A the contact area, which is much lower than the bonding energy of thiols 1 J/m^2 here.
[18] L. Bureau, C. Caroli, and T. Baumberger, Proc. R. Soc. A **459**, 2787 (2003).
[19] T. Brunet, X. Jia, and P. Mills, Phys. Rev. Lett. **101**, 138001 (2008).
[20] A. Laschitsch and D. Johannsmann, J. Appl. Phys. **85**, 3759 (1999).
[21] C. Redon, F. Brochard-Wyart, and F. Rondelez, Phys. Rev. Lett. **66**, 715 (1991).